Nanomed Res J 6(4):369-384, Autumn 2021

RESEARCH ARTICLE

Preparation, Characterization, Antimicrobial and Antitumor Activity of Chitosan Schiff base / PVA / PVP Au, Ag Nanocomposite in Treatment of Breast Cancer Cell Line

Baker F. Abdallaha [1*] ,Maha A.Younus [2],Ibraheem J. Ibraheem[1]

[1] Department of Chemistry, College of Science, University of Anbar, Ramadi, Iraq.

[2] Department of Chemistry / College of Education for Pure Science (Ibn Al-Haitham) / University of Baghdad / Iraq.

ARTICLE INFO

Article History:
Received 25 Aug 2021
Accepted 15 Oct 2021
Published 01 Nov 2021

Keywords:
Chitosan
Chitosan Schiff base
PVA
PVP
Nanocomposite
Antimicrobial
anticancer cell line

ABSTRACT

Objective(s): Biocompatibility, non-toxicity, minimal allergenicity, and biodegradability are all characteristics of chitosan. Other biological properties of chitosan have been reported, including antitumor, antimicrobial and antioxidant activities. This research aim is the synthesis of drug compounds by preparation and characterization of polymer chitosan Schiff base and chitosan Schiff base / Poly vinyl alcohol / poly vinyl pyrrolidone Nanocomposite and study applications (anticancer cell line, antimicrobial agents).

Methods: Chitosan Schiff base was prepared from the reaction of chitosan with carbonyl group of 4-nitro benzaldehyde. Polymer blend have been prepared by solution casting method. Chitosan Schiff base mixing with PVA and PVP. Green synthesis of AuNPs and AgNPs by onion peals extract as reducing agent. Nanocomposites were prepared by mixing 10 mL of chitosan Schiff base, 5 mL PVA and 5 mL of PVP with 25 mL of two different concentrations (100, 200 ppm) of AuNPs and AgNPs. In vitro bacterial activities polymer blends and Au, Ag nano composites were performed against pathogenic bacteria such as the *Acinetobacter baumannii, Staphylococcus aureus, Pseudomonas aeruginosa and Esherichia coli*. Cancer cell line (AMJ-13) cell line.

Results: The prepared AgNPs and AuNPs were characterized by UV-visible spectroscopy, SEM microscopy and XRD analysis. UV-vis spectrum of AuNPs at 543 nm and AgNPs at 425 nm, particles size of AuNPs 24.74 nm and AgNPs 18.77 nm. The polymer blends and nano composites were characterized by FT-IR, SEM, DSC and TGA. DSC analysis investigated the polymer blend and nano composites shows a good thermal stability for all prepared compounds. The inhibition zone of blend and nanocomposites The Inhibition zone of blend and Nano composites ranging between (8-15) millimetre with concentration of 20 mg. The inhibition rate of blend and Nanocomposites ranging between (1.33 – 77.33) for all compounds. IC 50 of blend and Nanocomposites ranging between (26.04- 183.56) µg for all compounds.

Conclusions: The prepared AgNPs and AuNPs were characterized by UV-visible spectroscopy, SEM microscopy and XRD analysis. UV-vis spectrum of AuNPs at 543 nm and AgNPs at 425 nm, particles size of AuNPs 24.74 nm and AgNPs 18.77 nm. The polymer blends and nano composites were characterized by FT-IR, SEM, DSC and TGA. DSC analysis investigated the polymer blend and nano composites shows a good thermal stability for all prepared compounds. The inhibition zone of blend and nanocomposites The Inhibition zone of blend and Nano composites ranging between (8-15) millimetre with concentration of 20 mg. The inhibition rate of blend and Nanocomposites ranging between (1.33 – 77.33) for all compounds. IC 50 of blend and Nanocomposites ranging between (26.04- 183.56) µg for all compounds.

How to cite this article
Abdallaha B.F., Younus M.A.,Ibraheem I.J. Preparation, Characterization, Antimicrobial and Antitumor Activity of Chitosan Schiff base / PVA / PVP Au, Ag Nanocomposite in Treatment of Breast Cancer Cell Line. Nanomed Res J, 2021; 6(4): 369-384.
DOI: 10.22034/nmrj.2021.04.007

* Corresponding Author Email: *baker.f.abdallaha@gmail.com*
fawzibaker7@uoanbar.edu.iq

INTRODUCTION

Biopolymers are polymeric biomolecules made up of monomeric components joined together by covalent bonds to form larger molecules. The term "bio" refers to materials that are biodegradable and produced by living creatures [1]. Chitosan a natural polysaccharide is widely utilized in pharmaceuticals, chitosan is produced from chitin and is found as a key component of fungus cell walls, crustacean and insect exoskeletons, and fish scales. It is a cationic polymer made up of (1–4) -2-amino-2-deoxy-glucan that has gotten more attention than chitin because of its pH sensitivity, biocompatibility and bioactive activities [2]. Schiff base derivatives of chitosan are one of the key changes and the newly generated imine groups increase the pharmacological effects of chitosan, such as anticancer, antibacterial and antioxidant activities [3]. Polymer blends are materials created by combining two polymers or copolymers to create a new material with characteristics that complement each other [4]. PVP, also known as povidone or polyvidone is a biocompatible and non-toxic polymer that has been recognized as safe by the Food and Drug Administration. PVP is one of the most promising polymers for nano gel production. Water solubility, toxicity loss, film formation, and adhesive strength are some of its adaptable properties [5]. PVA is a non-toxic, water soluble synthetic polymer with strong physical and chemical characteristics as well as film forming capabilities. PVA is bio inert and it has a variety of applications in medicine, including hemodialysis, nano filtration and composite films. When compared to the characteristics of the individual components, chitosan Schiff base, PVA and PVP give benefits in terms of stability, mechanical strength, and bio compatibility [6]. Nanoparticles have received attention in extensive modern research fields, including electronics, sensors, and medicine. Many different Metal nano particles, such as silver (AgNPs), gold (AuNPs), have been synthesized and investigated in various ways including photochemical synthesis, electrochemical and reduction of solution [7]. Green synthesis aims to avoid producing products that are harmful to the environment through a reliable, sustainable and eco-friendly synthesis process. Therefore, in the green synthesis of metal nanoparticles, microorganisms (e.g. bacteria and fungi) and plant extracts (e.g. root, flower, and fruit) are used as reducing agents, the process for making MNPs from biological materials is easy, economical, environmentally friendly, low-energy, non-toxic and stable [8]. Chitosan nanoparticles have three active hydroxyl groups, a primary and one secondary hydroxy group for each repeated unit, and one amino group for each desacidstylized unit. Chitosan nanoparticles are a hydrophilic polymer with a positive charge. The main factors that affect the adsorption capacity of nano chitosan are its particle size, surface area, molecular weight and degree of deacetylation [9]. Nanocomposites have been utilized in a variety of applications, including wound healing, tissue engineering, thermal treatment and drug delivery. Nanocomposites offer a variety of qualities that make them suitable, including mechanical and thermal capabilities, as well as antibacterial properties [10]. In this work, chitosan nanocomposite with metals (gold and silver) have been prepared, due of its organic application properties, chitosan and chitosan derivatives, particularly those produced through a Schiff base reaction, are the most significant. Recently, the interaction of chitosan with aromatic compounds resulted in the effective synthesis of stable Schiff bases, which are remarkable molecules in many fields of pharmacology and medicine, such as antibacterial and cancer prevention agents [11]. The pH of the environment, the molecular weight of the chitosan and the degree of acetylation of the chitosan have all been shown to influence the amount of chitosan binding to the bacterial cell wall. Low pH in the environment increases the positive charge in the chitosan polymer which facilitates bacterial cell wall binding. [12]. Cancer is a malignant neoplasm illness caused by aberrant and uncontrolled cell development. It is the second leading cause of mortality globally behind heart disease. Its nature is classified as the most hazardous kind of cell proliferation with diverse abnormalities [13].

METHODS

Chitosan Schiff base preparation (Cs)

Chitosan (0.5gm) was dissolved in acetic acid 2% and stirred for 1 hour at temperature 60 ˚C, 4-nitro benzaldehyde (1gm) was dissolved in 30 ml ethanol and stirred for 30 minutes at room temperature and mixing all materials to prepare graft polymer. The mixture was magnetically stirred and heated at a temperature of 60 ˚C for 18 hours with reflex. After cooling, the crude product was washed with ethanol. The product was dried at

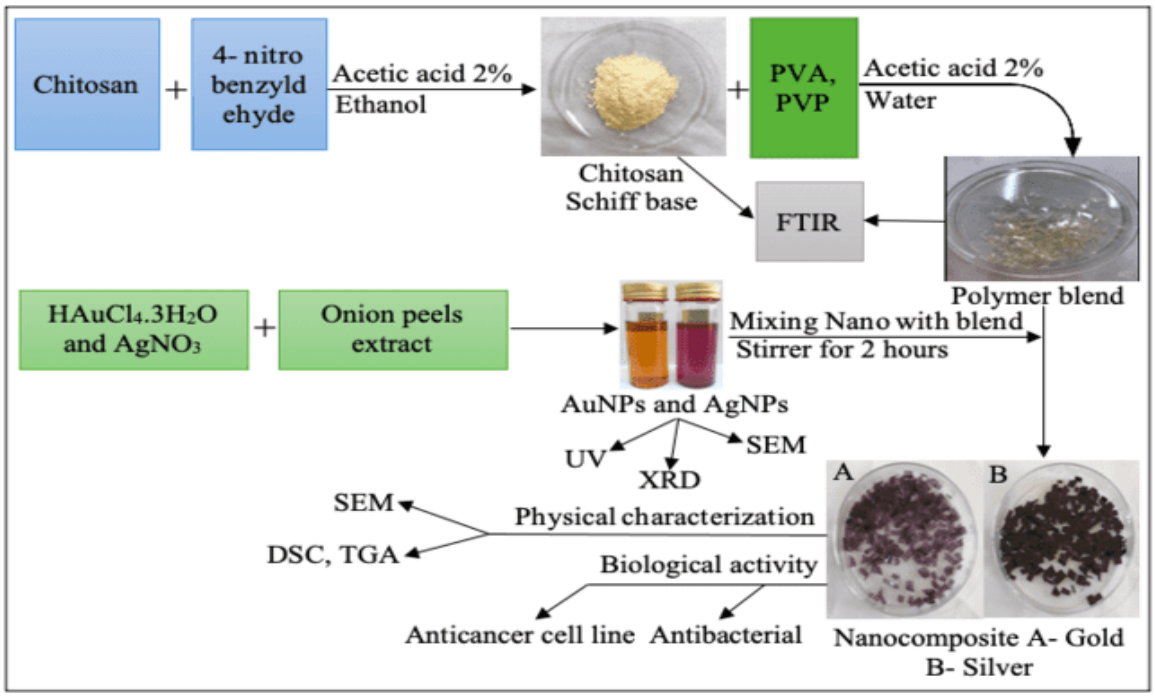

Fig. 1. General scheme of preparation Nano composites

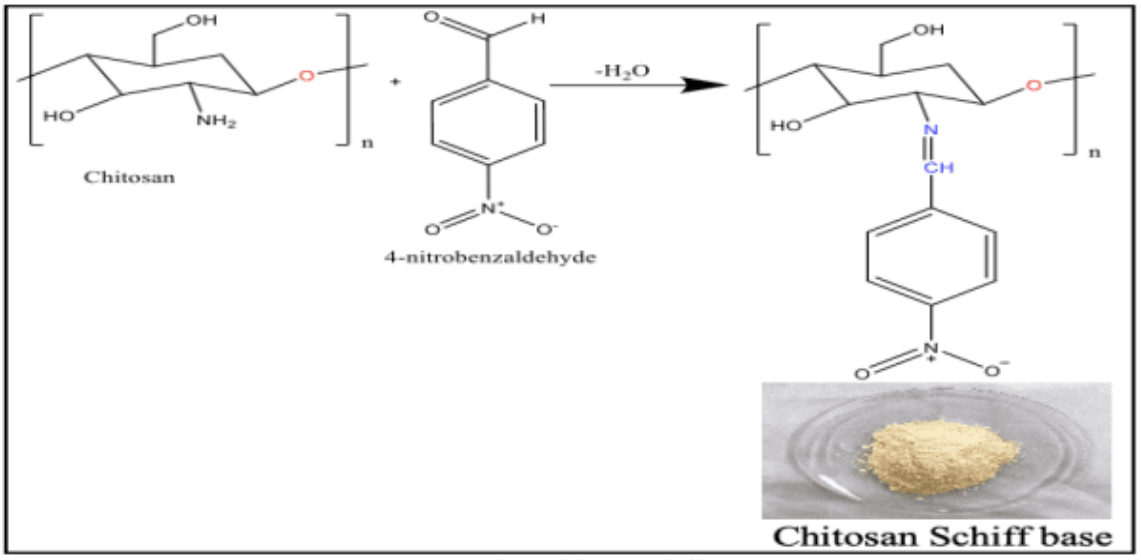

Fig. 2. Synthesis of chitosan Schiff base.

50 ˚C in oven for 24 hours [14]. The synthetic route of chitosan Schiff base is shown in (Fig. 2).

Polymer Blend Preparation

Polymer blends have been prepared by solution casting method, chitosan Schiff base solution was prepared by dissolution 1 gm of the of Chitosan Schiff base in 2% solution of aqueous acetic acid 50 ml with stirring for 1hour at 60 ˚C, (5gm) of PVA and PVP have been dissolved in 50 ml of water in order to prepare 10 wt % solutions of the polymer,10 ml Cs, 5 ml PVA and PVP polymer solutions have been mixed to make homogenous solution using hotplate stirrer for 30 minutes. To

make the film, the combination solution was cast on Petri-dishes and dried in an oven at 50 ˚C for 24 hours. Cs / PVA / PVP blends were prepared by mixing different ratio Cs: PVA: PVP (10:5:5) [15].

Green synthesis of Au and Ag Nano particles
Preparation of crude extract (Onion peels)

Deionized water (100 mL) was added to 10 gm of leaf powder to prepare the onion peels extract. The mixture was stirred and heated at 50 ˚C for 2 hours, and the resultants were filtered and dried in oven at 50 ˚C temperature. (0.01gm) of powder product was dissolved in 100 ml deionized water to get onion peels extract (100 ppm). As a stabilizing and reducing agent, fresh extract made from onion peels was utilized. [16].

Preparation of $HAuCl_4.3H_2O$, $AgNO_3$ solutions

Gold chloride trihydrate ($HAuCl_4.3H_2O$) (1gm) was dissolved in 100 mL of deionized water to prepare the stock solution, after (2 mL) was taken from stock solution and completed to 100 ml by applying sequential dilution operations to have (100 ppm). $AgNO_3$ was synthesis by dissolving (0.016gm) of $AgNO_3$ in 100 ml deionized water also to have (100 ppm).

Green synthesis of Au and Ag nanoparticles

Aqueous onion peels extract (3 mL) was added to (10 mL) of aqueous gold chloride solution and silver nitrate with sequence, the final mixture was stirrer for 10 minutes at 25 ˚C [17]. The gold color changed from yellow to purple which confirms the formation of AuNPs, The color of silver was altered from colorless to brown, indicating that AgNPs had formed, The process of separating the nanoparticles is carried out by a centrifuge (10000 rpm) to separate the precipitate from the filtrate, then the precipitate is taken, collected and dilute with deionized water [18].

Preparation of Cs / PVA / PVP Gold and Silver Nanocomposites

Nanocomposites were prepared by mixing 10 mL of chitosan Schiff base, 5 mL PVA and 5 mL of PVP with 25 mL of two different concentrations (100, 200 ppm) AuNPs and AgNPs with sequence and stirred for 2 hours, the mixture solution was cast onto Petri-dishes and kept in a constant temperature oven at 50 ˚C in oven for 24 hours to obtain the nanocomposite film [19]. As shown in (Fig. 3).

Antimicrobial activity

In vitro bacterial activities polymer blends and Au, Ag nano composites were performed against pathogenic bacteria such as the *Acinetobacter baumannii*, *Staphylococcus aureus*, *Pseudomonas aeruginosa*, and *Esherichia coli* were collected from Anbar University's Department of Biology, College of Science, where their sensitivity to common antibiotics was also examined by using disk diffusion method. The clear zone of inhibition was measured using Muller-Hinton agar and the agar well diffusion technique. The concentration of polymer blend and nanocomposite were 20 mg. The discs have been placed on seeded plates and incubated for 24 hrs at a temperature of 37 ˚C. The diameters of inhibition zone which surrounds every disc have been evaluated after (24) hours [20].

Anticancer Activity
Cell Cultures

The cells were cultured in RPMI-1640 medium with 10% Fetal bovine serum, 100 units/mL penicillin and 100 g/mL streptomycin. Cells were passaged with Trypsin-EDTA twice a week and

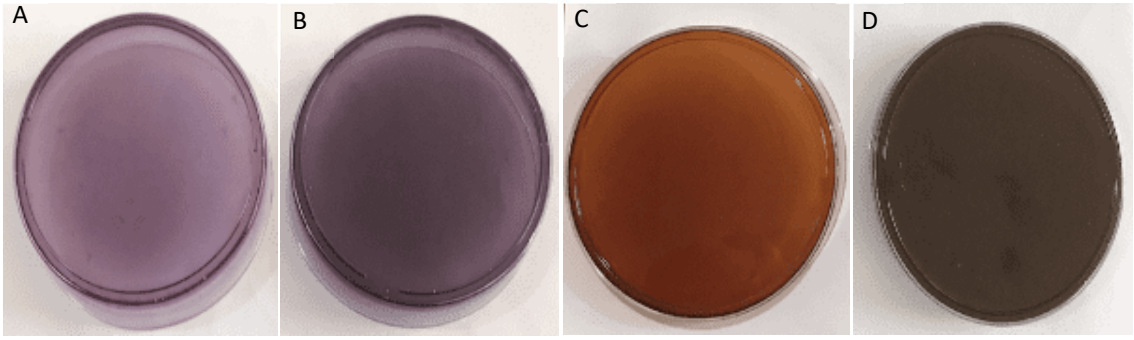

Fig. 3. Nanocomposites (A- Cs / PVA / PVP Nano Au 100 ppm), (B- Cs / PVA / PVP Nano Au 200 ppm), (C- Cs / PVA / PVP Nano Ag 100 ppm), (D- Cs / PVA / PVP Nano Ag 200 ppm).

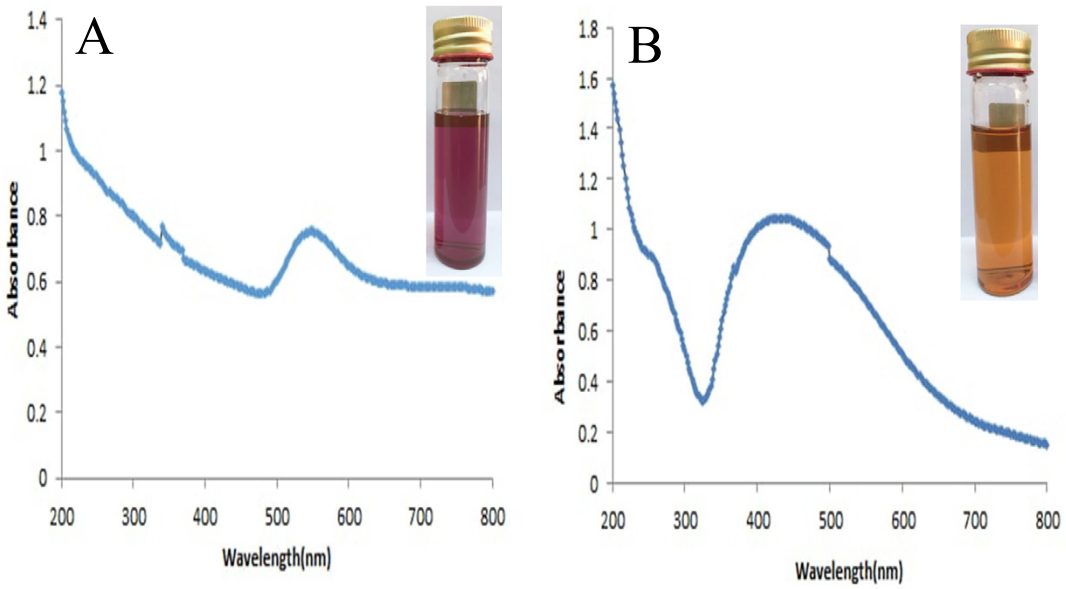

Fig. 4. UV-vis spectrum of (A-AuNPs) and (B- AgNPs)

reseeded when they reached 80% confluence. [21, 22].

Cytotoxicity Assays

Cancer cell line (AMJ-13) cell line were obtained from the cancer research center in Baghdad. the MTT test was used in 96-well plates to assess the cytotoxic impact of polymer blends and nanocomposites [23, 24]. After 24 hours, or after a confluent monolayer had formed, cells were treated with the tested chemicals at various doses and cell viability was assessed. After 72 hours of treatment, the vitality of the cells was determined by removing the medium, adding 28 liters of a 2 mg/mL MTT solution and incubating the cells for 2.5 hours at 37 °C. After the MTT solution was withdrawn, the crystals in the wells were solubilized by adding 130 µL of DMSO (Dimethyl Sulphoxide) and incubating at 37 °C for 15 minutes with shaking. [25]. The absorbency was measured at 492 nm using a microplate reader and the experiment was carried out three times. The following equation was used to compute the rate of cell growth inhibition (the percentage of cytotoxicity): [26, 27] (Inhibition rate = A- B/A*100), where A is the optical density of the control and B is the optical density of the sample. [28].

The cells were seeded at a density of $1*10^5$ cells ml^{-1} into 24-well micro-titration plates and grown for 24 hours at 37 ˚C to check their shape under an inverted microscope. Polymer blends and Nano composites were exposed to cells at their IC50 concentration for 24 hours. After the exposure time, the plates were stained with crystal violet dye and incubated at 37 ˚C for 10-15 minutes. The dye was carefully washed out of the stain with tap water until it was completely gone. The cells were shot at a magnification of 100 x using a digital camera attached to an inverted microscope [29, 30, 31].

RESULTS AND DISCUSSION

Characterization of AuNPs and AgNPs.

The preparation AuNPs and AgNPs were characterized by UV-Vis spectroscopy (INOVIALAB-1911DB, China), SEM microscopy (TESCAN Czech Republic), X-ray Powder Diffraction (XRD) (Malvern Panalytical), FTIR (IRAFFINITY-1SHIMHDSO JUPAN), DSC, TGA (Q600).

Spectroscopy in the ultraviolet and visible ranges (UV-Vis)

The UV-Vis spectrum of AuNPs and AgNPs solution is given in (Fig. 4) UV-vis spectroscopy is a method that may validate the production of metal nanoparticles in aqueous solution, (Fig.4) B showed the UV-vis spectra of AgNPs solution, with a broad surface plasmon resonance (SPR) band appearing at 425 nm, indicating the creation of

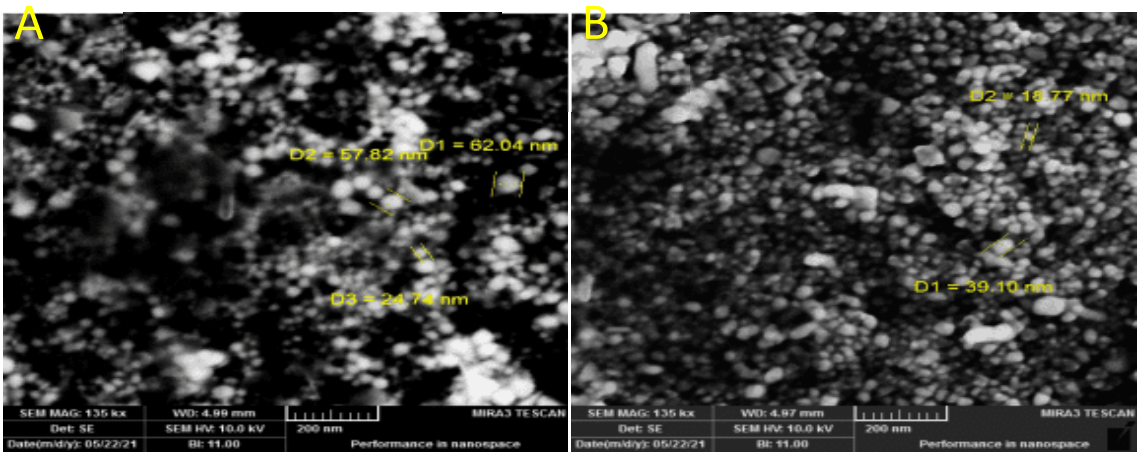

Fig. 5. Scanning Electron Microscopy of (A- AuNPs) and (B- AgNPs).

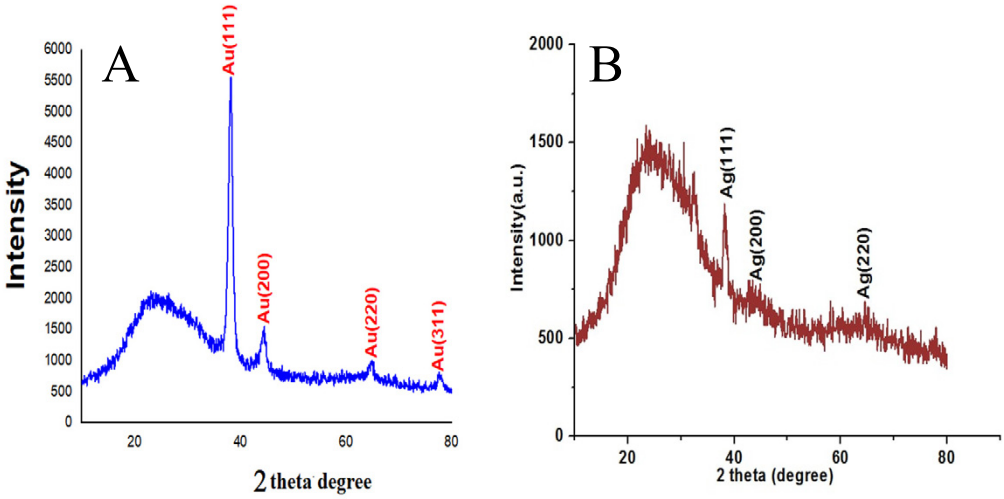

Fig. 6. XRD Patterns of (A- AuNPs) and (B- AgNPs).

AgNPs. (Fig. 4) A showed the UV-vis spectrum of AuNPs solution with a broad (SPR) band appearing at 543 nm, showing the formation of AuNPs [32]. The (SPR) of AgNPs and AuNPs was used to explain the interaction between free electrons on the metal surface and incoming light. [33, 34].

Scanning Electron Microscopy

The average size and morphology of nanoparticles in the test sample may be determined using SEM imaging, which is an analytical method [35]. (Fig. 5) A,B shows a typical surface of AgNPs and AuNPs prepared from onion peels using green synthesis. The SEM picture revealed a shape of gold Nanoparticles that formed with diameter ranges from (24.74, 57.82, 62.04) nm, the SEM picture revealed a shape of silver nanoparticles that formed with diameter ranges from (18.77, 39.10) nm.

Analysis of X-ray diffraction (XRD)

X-ray diffraction (XRD) analysis was used to assess the crystalline nature of prepared AgNPs and AuNPs. (Fig. 6) A, B and Table 1 are showing the XRD data of produced AuNPs and AgNPs. Both dried AuNPs and AgNPs had a 2theta degree of 10 to 80. Sharp strong peaks were detected at 38°, 44°, 64°, and 77° for AuNPs, which corresponded to the Braggs planes (111), (200), (220), and (311), respectively, according to (JCPDS 04-0784) [36]. confirming that the produced AuNPs possessed a face-centered cubic structure. For AgNPs, the peak obtained at 2theta values 38°, 44°, and 64° correspond to Braggs reflection (111), (200) and (220) respectively, according to (JCPDS 04-0783) [37].

Table 1 XRD examination of AuNPs and AgNPs yielded calculated crystallite sizes for all allocated and D average peaks.

Element	2 theta	FWHM	Hkl	Average	D average
Au	38.2	0.59	111	3.11nm	
	44.4	0.49	200	4.12nm	3.96 nm
	64.9	0.78	220	4.27nm	
	77.7	0.78	311	4.36nm	
Ag	38.09	0.49	111	3.74nm	
	44.2	0.3	200	6.79 nm	3.97 nm
	63.91	3.14	220	1.04nm	

Characterization of chitosan, chitosan Schiff base and blend

FTIR Analysis

(Fig. 7) A, represents the FT-IR spectrum for chitosan assigned as follows. The broad band at (3267) cm^{-1} corresponding to (NH and OH stretching vibration), 2920 cm^{-1} is due to (C-H symmetric stretch), (1621, 1546) cm^{-1} assigned to amide I, 1369 cm^{-1} (NH_2 bending vibration), 1145 cm^{-1} (C–O–C bending vibration) and 1061 cm^{-1} (C–OH stretching vibration), (Fig. 7) B showed a new absorption band at 1647 cm^{-1} attributed to (C=N) of imine group, The absorption at 1520 cm^{-1} assigned for the C=C of 4- nitro benzaldehyde, the peak appeared at 810 cm^{-1} linked to the aromatic range's C-H deformation because stretching vibration of (C–O–C) pairing in β (1-4) glycosidic bonds, additional peaks emerged at 1099 cm^{-1}, For the prepared polymer blend (Fig. 7) C showed a broad band around 3321cm^{-1} attributed to stretching vibration of hydroxyl group (OH^-) of PVA and the secondary amide (–NH)of un reacted chitosan, the band at around 1022 cm^{-1} indicates the presence of (OH) hydroxyl group with polymeric association and (–NH) a secondary amide, also band appeared at 1427 cm^{-1} assigned to pyridine ring (C=N) [38].

Scanning Electron Microscope

Surface morphology, size, crystallinity and phase locations of the produced material may all be studied via SEM examination. [39]. The surface morphology changes for the prepared polymer, chitosan, chitosan Schiff base, polymer blends and polymer nano composite were studied using SEM technique, SEM micrograph for chitosan, chitosan Schiff base / PVA / PVP nano-composite loaded with nano-particles of Au, Ag have been depicted in (Fig. 8)

Thermal Analysis (TGA, DSC)

The Thermo Gravimetric Analysis and Differential Scanning Calorimeter (TGA, DSC) for, chitosan, chitosan Schiff base, chitosan Schiff base / PVA / PVP polymer blend and Chitosan Schiff base / PVA / PVP Au, Ag nanocomposite have been measured in temperature range between 25 ˚C and 1000 ˚C with a constant rate which is equal to 10 ˚C / min.

TGA curve of chitosan (Fig. 9) A illustrated three stages of a sequence mass lose, the first stage with mass lose (-7.368%) of volatile compounds. The second-step with weight loss approximately (-44.21%) for the side group decomposition, the third stage with weight loss of approximately (-37.46%) for the chain decomposition [40]. DSC curve in the (Fig. 9) A° for chitosan showed a Tg of (85.43 ˚C). Peak at (317.75 ˚C) regarding to the polymer melting Tm [41]. TGA curve of chitosan Schiff base (Fig. 9) B illustrated six stages of a sequence mass lose, the first stage with mass lose (-4.396%) of volatile compounds. The second-step with weight loss approximately (-37.99%), the third stage with weight loss of approximately (-6.437%), the forth stage with weight loss of approximately (-13.90%), the fifth stage with weight loss of approximately (-6.27%), the sixth stage with weight loss of approximately (-16.73%) [40]. DSC curve in the (Fig. 9) B° for chitosan Schiff base showed a Tg of (56.12 ˚C). peak regarding to the crystalline temperature point Tc at (274.72 ˚C). Peak at (477.76 ˚C) regarding to the polymer melting Tm [41].

TGA curve of Chitosan Schiff base / PVA / PVP polymer blend figure (Fig. 9) C illustrated four stages of a sequence mass lose, the first stage with mass lose (-3.529%) of volatile compounds. The second-step with weight loss approximately (-15.53%), the third stage with weight loss of approximately (-63.37%), the forth stage with weight loss of approximately (-9.131%) [40]. DSC curve in the (Fig. 9) C° for Chitosan Schiff base / PVA / PVP polymer blend showed a Tg of (112.12 ˚C). peak regarding to the Crystalline temperature point Tc at (268.49 ˚C). Peak at (449.86 ˚C) regarding

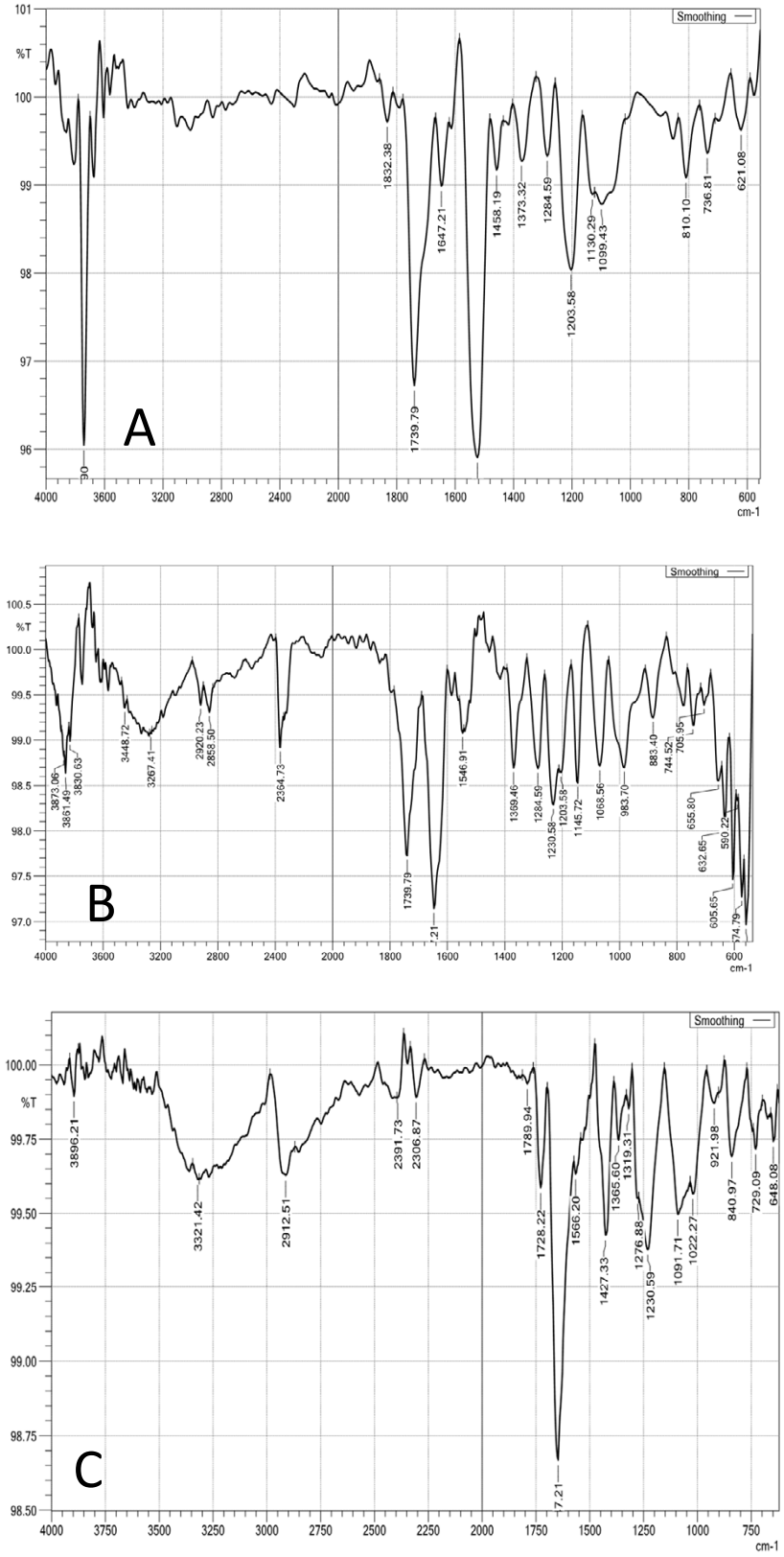

Fig. 7. FTIR Spectrum (A- Chitosan), (B- Chitosan Schiff base), C-Blend (Cs, PVA, PVP)

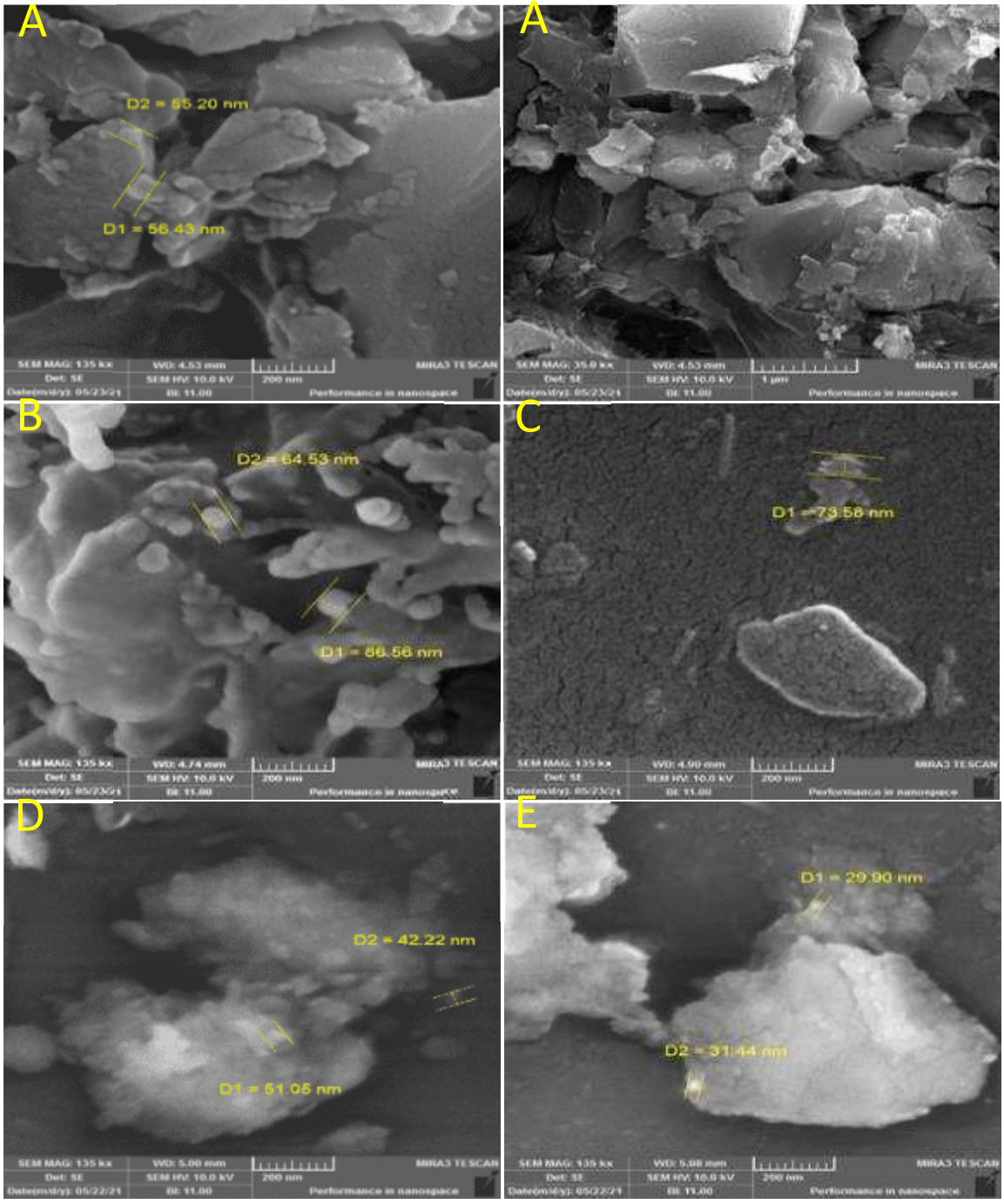

Fig. 8. SEM images (A- Chitosan 200 nm,1µm), (B- Chitosan Schiff base), C- Blend (Cs, PVA, PVP), D- Nanocomposite (Cs, PVA, PVP and Nano gold), E- Nano composite Cs, PVA, PVP and Nano silver)

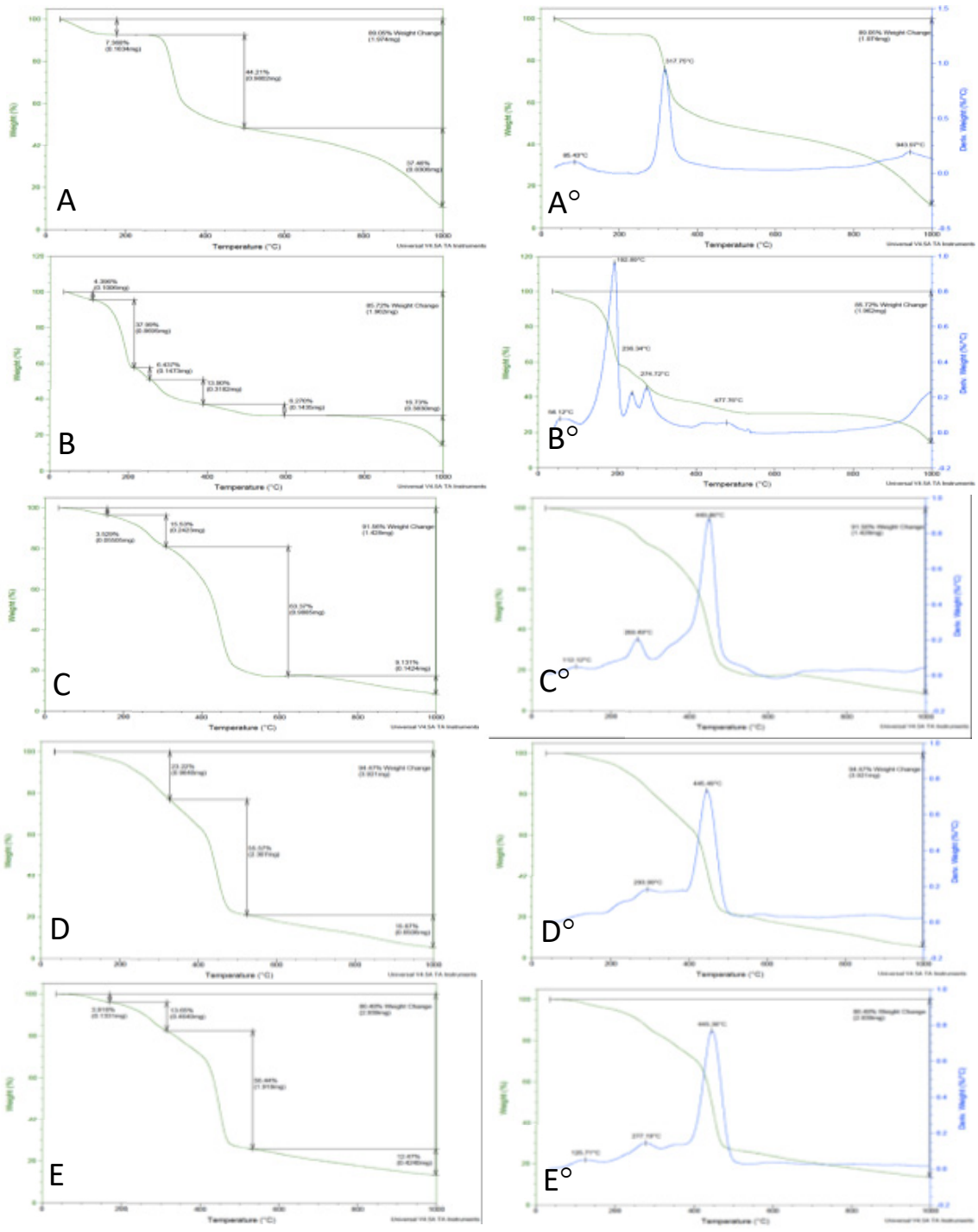

Fig. 9. Thermal analysis (TGA,DSC) (AA°- Chitosan), (BB°- Chitosan Schiff base), (CC°-Blend (Cs, PVA,PVP)), (DD°- Nanocomposite (Cs, PVA, PVP and Nano gold)), (EE°- Nano composite (Cs, PVA, PVP and Nano silver))

to the polymer melting Tm [41].

The TGA curve of chitosan Schiff base / PVA / PVP-Au nanocomposite (NC-Au) (Fig. 9) D illustrated three stages of a sequence mass lose , the first stage with mass lose (-23.22%) of volatile compounds. The second stage with weight loss approximately (-55.57%), the third stage with weight loss of approximately (-15.67%) for the chain decomposition [40]. DSC curve in the (Fig. 9) D° for NC-Au showed Crystalline temperature point Tc at (293.99 ˚C). Peak at (445.49 ˚C) regarding to the polymer melting Tm [41].

The TGA curve of chitosan Schiff base / PVA / PVP-Ag nanocomposite (NC-Ag) (Fig. 9) E illustrated four stages of a sequence mass lose , the first stage with mass lose (-3.916%) of volatile compounds. The second stage with weight loss approximately (-13.65%), the third stage with weight loss of approximately (-56.44%), the fourth stage with weight loss of approximately (-12.47%) for the chain decomposition [40]. DSC curve in the (Fig. 9) E° for NC-Ag showed a Tg of (125.71 ˚C), peak regarding to the Crystalline temperature point Tc at (277.19 ˚C). Peak at (445.36 ˚C) regarding to the polymer melting Tm [41].

All temperatures are shifted slightly toward a higher temperature, indicating the influence of the coordination bonding of gold &silver on thermal stability, also it was observed that the blend film show only one Tg as shown on its thermo gram. This indicates the presence of hydrogen bonding interactions between Cs, PVA and PVP in the blend and that these three polymers are well blended together. These findings indicate that the addition of Nano-Au & Ag at such an exceptionally low concentration can improve the thermal stability of Cs/PVA/PVP nanocomposite.

Antibacterial activity

Chitosan is well reported biocompatible and antimicrobial polymer used in various applications. The biological activity of polymer blends, chitosan Schiff base / PVA / PVP /Au, Ag nano composite and antibiotic were tested against four kinds of pathogenic bacteria (Gram +ve and Gram -ve) using Disk Diffusion inhibition method [42]. The results of antibacterial activity and antibiotic were represented in Table 2, 3. The antibacterial properties of chitosan Schiff base, which may be linked to the chemical structure of the studied microorganisms, the presence of the Schiff-base molecule's imine group (C=N) with its π - electrons is thought to improve the molecule's lipophilicity making it easier for it to enter the microbe's cell membrane. The antibacterial activity mechanism of nanoparticles differs significantly from that of conventional biocides. The contact of nanoparticles with the cellular membrane is the most essential contribution of nanoparticles in the biocidal process, due to their incredibly tiny size and capacity to permeate it. After that, nanoparticles release reactive species by reacting

Table 2 Inhibition zone diameter in millimetre for the blends and Nanocomposite polymers.

Compounds	Inhibition zone diameter (millimetre)			
	Pseudomonas aeruginosa	***Acinetobacter baumannii***	***Staphylococcus aureus***	***Esherichia Coli***
PB	R	R	11± 0.42	R
NC-Au_1	R	R	15± 0.61	8± 0.28
NC-Au_2	R	R	13± 0.47	R
NC- Ag_3	13± 0.52	12± 0.49	12± 0.45	11± 0.45
NC- Ag_4	13± 0.54	10± 0.38	10± 0.35	15± 0.62

R: Resistant, PB: polymer blend, NC-Au_1: Nanocomposite gold (100 ppm), NC-Au_2: Nanocomposite gold (200 ppm), NC-Ag_1: Nanocomposite silver (100 ppm), NC-Ag_2 Nanocomposite silver (200 ppm), (Mean±S.D.)

Table 3 Antibiotic activity towards pathogenic bacterial

Antibiotic	Symbol	Inhibition zone diameter (millimetre)			
		Pseudomonas aeruginosa	***Acinetobacter baumannii***	***Staphylococcus aureus***	***Esherichia Coli***
Doxycycline	DXT	20± 0.63	18± 0.47	19± 0.51	13± 0.32
Piperacillin	PTZ	30± 0.82	25± 0.77	28± 0.77	21± 0.54
Imipenem	IMI	23± 0.58	21± 0.63	23± 0.64	22± 0.58
Tobramycin	TN	18± 0.48	15± 0.41	15± 0.42	R
Cefepime	CPM	28± 0.79	22± 0.55	21± 0.52	11± 0.34

R: Resistant, (Mean±S.D.)

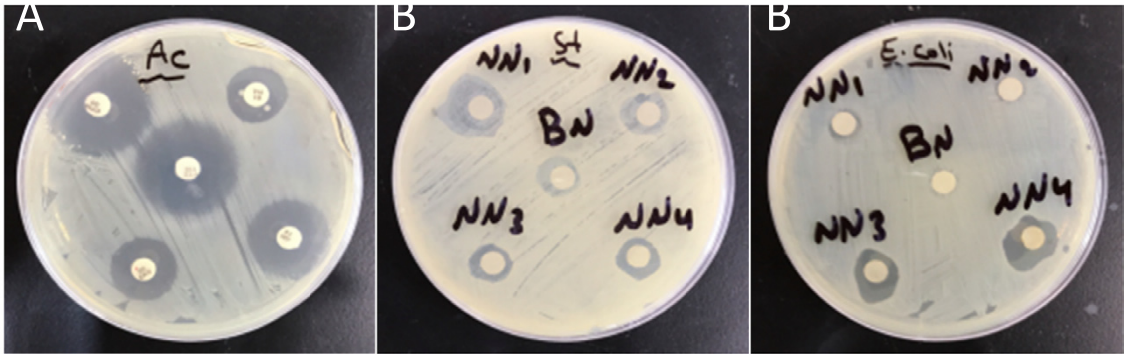

Fig. 10. A- Antibiotics B- BN: Polymer Blend, NN_1 (Nanocomposite gold 100 ppm), NN_2 (Nanocomposite gold 200 ppm), NN_3 (Nanocomposite silver 100 ppm), NN_4 (Nanocomposite silver 200 ppm)

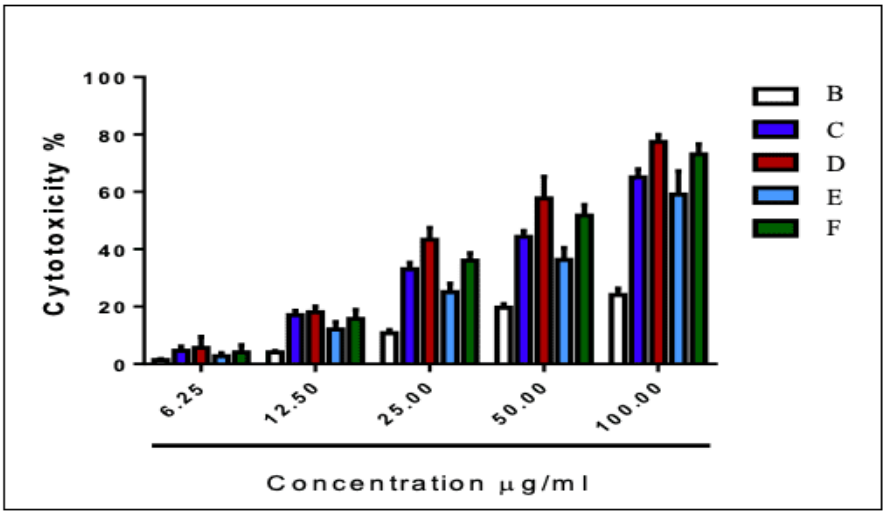

Fig. 11 Cytotoxic effect of blend and nano composites (gold, silver) B-AMJ-13 cells undergo after being treated with blend. C-AMJ-13 cells after being treated with (NC/Au100 ppm). D-AMJ-13 cells after being treated with (NC/Au 200 ppm). E-AMJ-13 cells after being treated with (NC/Ag100 ppm). F-AMJ-13 cells after being treated with (NC/Ag 200 ppm)

with the cells' inert environment [43]. Ionic or free radical threats that target enzymes and DNA in the cellular nucleus, causing microbial death or growth inhibition are examples of reactive species [44]. The Inhibition zone of polymer blend and nanocomposites as shown in (Fig. 10). Previous studies, on the other hand, have looked at a variety of ways and substances that can be utilized to inhibit pathogenic bacteria, such as the direct effect of Ag and TiO2 nanoparticles on pathogenic bacteria like *Proteus mirabilis* and *Proteus vulgaris* [45]. Using physical forces therapy on dangerous bacteria, such as Audible Sounds and Magnetic Fields, has been shown in several trials to help diminish *S. aureus* infection resistance [46].

Anticancer cell line

The cytotoxic effect of blend, Nanocomposites against cancercells was studied. The capacity of the blend, Nanocomposites, to suppress the growth of the breast cancer cell line AMJ-13 was used to assess their anticancer efficacy. The results of this research revealed that blend, nanocomposites had extremely substantial cytotoxic effect against human cancer cell lines. As shown in Fig. 12. The findings show that blends, nanocomposites have the capacity to inhibit the development of cell lines and that this impact is concentration dependent. Inhibition rate and viability of cells of blend and nano composites showed in Table 4. The results showed nanocomposites more inhibitor compared with blend. The results showed cytotoxic effect in AMJ13 cells, IC50 of B = 183.56 µg\ml, IC50 of C =37.78 µg\ml, IC50 of D = 26.04 µg\ml, IC50 of E = 42.61µg\ml, IC50 of F = 35.57 µg\ml [47]. As shown in Fig. 11.

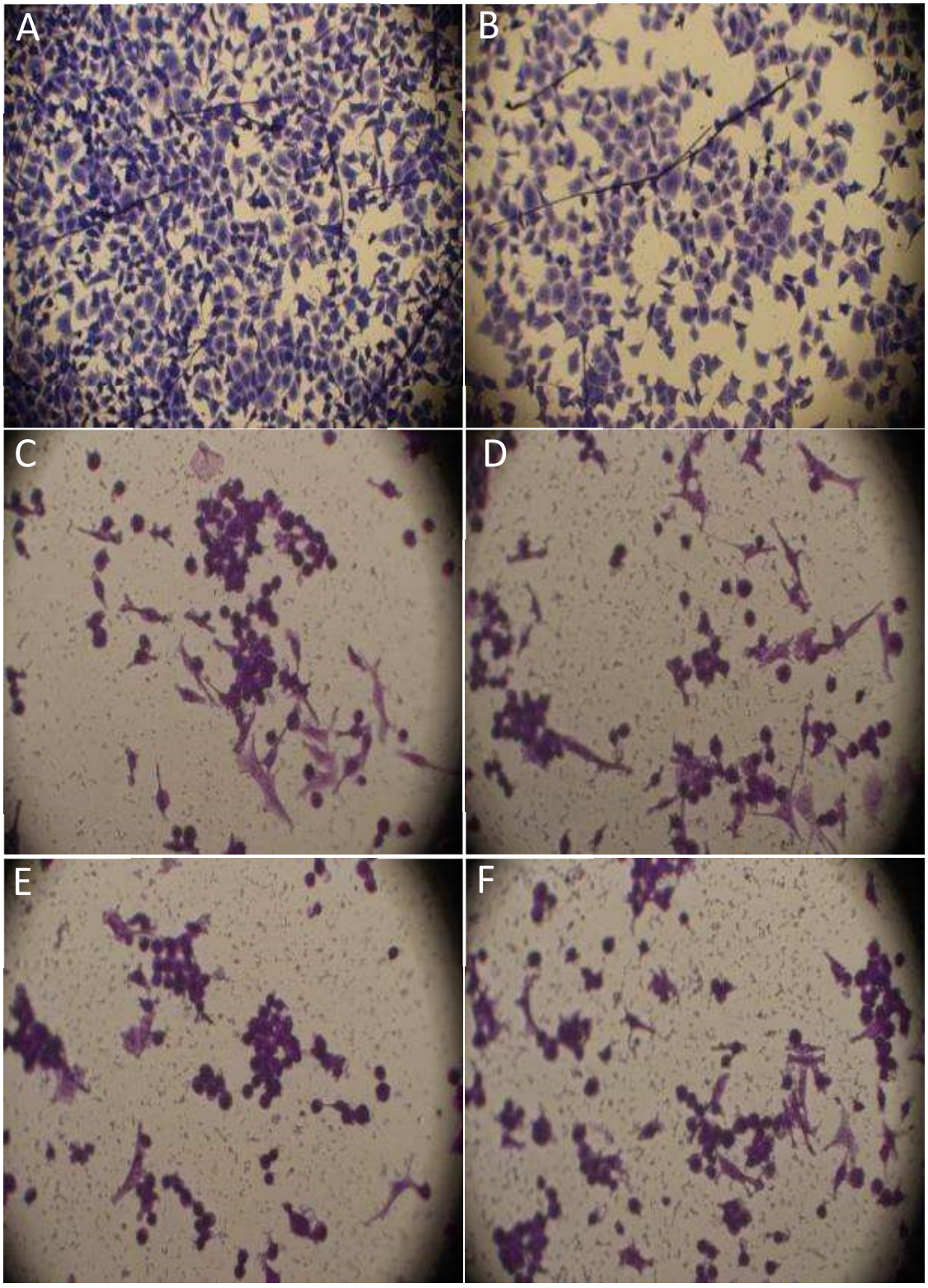

Fig. 12. Breast cancer cells images before and after treatment A- Control untreated AMJ-13 cells. B-AMJ-13 cells after being treated with blend. C-AMJ-13 cells after being treated with (NC/Au 100 ppm). D-AMJ-13 cells after being treated with (NC/Au200 ppm). E-AMJ-13 cells after being treated with (NC/Ag 100 ppm). F-AMJ-13 cells after being treated with (NC/Ag 200 ppm).

Table 4 Inhibition rate and viability of cells of blend and nano composites for chitosan Schiff base (4. Nitro Benzaldehyde)

No.	Symbol	Samples	Concentration	Inhibition rate	Viability of cells
1	B	Blend	6.25	1.33	98.67
			12.5	4	96
			25	10.66	89.34
			50	19.66	80.34
			100	24	76
2	C	Nano composite Gold (100 ppm)	6.25	4.66	95.34
			12.5	17	83
			25	33	67
			50	44.33	55.67
			100	65	35
3	D	Nano composite Gold (200 ppm)	6.25	5.66	94.34
			12.5	18	82
			25	43.33	56.67
			50	57.66	42.34
			100	77.33	22.67
4	E	Nano composite Silver (100 ppm)	6.25	2.66	97.34
			12.5	12	88
			25	25	75
			50	36.33	63.67
			100	59	41
5	F	Nano composite Silver (200 ppm)	6.25	4	96
			12.5	15.66	84.34
			25	36	64
			50	51.66	48.34
			100	73	27

CONCLUSION

Chitosan Schiff base Cs, Cs / PVA / PVP polymer blend, Cs / PVA / PVP-Au, Ag nanocomposites were prepared. In these synthetic methods, onion peels were used as a reducing and stabilizing agent, UV-vis spectra revealed a characteristic SPR band of 543 nm for AuNPs and 425 nm for AgNPs, and XRD data assessed the crystallinity of these produced nanoparticles. Both AuNPs and AgNPs were face-centered cubic, with average crystallite diameters of 3.96 nm for AuNPs and 3.97 nm for AgNPs for the assign peaks. Addition of AuNPs, AgNPs increasing the biological activity, chitosan Schiff base, polymer blends, Nanocomposites shown activity towards pathogenic bacterial (gram $_{+}$ve and gram -ve), chitosan Schiff base show more activity than polymer blend, Nanocomposites shown more anticancer activity than polymer blend due existence Au, Ag nanoparticles which increasing activity towards breast cancer cell line AMJ-13.

ACKNOWLEDGMENTS

The authers would like to acknowledge the contribution of the University of Anbar (www.uoanbar.edu.iq) via their prestigious academic staff in supporting this research with all required technical and academic support.

CONFLICTS OF INTEREST

The authors declare that there are no conflicts of interest.

REFERENCES

[1] Hernández, N., Williams, R. C., and Cochran, E. W. "The battle for the "green" polymer. Different approaches for biopolymer synthesis: bio advantaged vs. bio replacement". Organic and biomolecular chemistry, (2014). 12(18), 2834-2849.

[2] Yanat, M., & Schroën, K. Preparation methods and applications of chitosan nanoparticles; with an outlook toward reinforcement of biodegradable packaging. Reactive and Functional Polymers, (2021). 104849.

[3] Antony, R., Arun, T., Manickam, S.T.D. A review on applications of chitosan-based Schiff bases. International Journal of Biological Macromolecules, (2019).129, 615-633.

[4] Utracki, L. A., and Wilkie, C. A. (Eds.). *"Polymer blends handbook"* Dordrecht: Kluwer academic publishers. (2002). (Vol. 1, p. 2).

[5] Aboelwafa, M. A., Abdelghany, A. M., & Meikhail, M. S. Preparation, Characterization, and Antibacterial Activity of ZnS-NP's Filled Polyvinylpyrrolidone/Chitosan Thin Films. Biointerf. Res. Appl. Chem., (2021). 11(6), 14336-14343.

[6] Saeedi, F., Montazeri, A., Bahari, Y., Pishvaee, M., & Ranjbar, M. Synthesis and Characterization of Chitosan-Poly Vinyl Alcohol-Graphene Oxide Nanocomposites. International Journal of Chemoinformatics and Chemical Engineering (IJCCE), (2018). 7(1), 1-12.

[7] Kim, B., Song, W. C., Park, S. Y., & Park, G. Green Synthesis of Silver and Gold Nanoparticles via Sargassum serratifolium Extract for Catalytic Reduction of Organic Dyes. Catalysts, (2021). 11(3), 347.

[8] Rauf, A., Ahmad, T., Khan, A., Maryam, Uddin, G., Ahmad, B., ... & Al-Harrasi, A. Green synthesis and biomedicinal applications of silver and gold nanoparticles functionalized with methanolic extract of Mentha longifolia. Artificial Cells, Nanomedicine, and Biotechnology, (2021). 49(1), 194-203.

[9] Mohammed, A. J., & Jasim, B. E. Nano Chitosan Adsorption Of Yellow (W6GS) Dye. NVEO-NATURAL VOLATILES & ESSENTIAL OILS Journal| NVEO, (2021). 6734-6743.

[10] Shabunin, A. S., Yudin, V. E., Dobrovolskaya, I. P., Zinovyev, E. V., Zubov, V., Ivan'kova, E. M., &Morganti, P. Composite wound dressing based on chitin/chitosan nanofibers: processing and biomedical applications. Cosmetics, (2019). 6(1): 1-10.

[11] Haj, N. Q., Mohammed, M. O., & Mohammood, L. E. Synthesis and biological evaluation of three new chitosan Schiff base derivatives. ACS omega, (2020). 5(23), 13948-13954.

[12] Rhoades, J., and Roller, S. "Antimicrobial actions of degraded and native chitosan against spoilage organisms in laboratory media and foods". Applied and environmental microbiology, (2000). 66(1), 80-86.

[13] Al-Shakarchi, Wejdan. The co-administration of anticancer and pro-apoptotic agents as a novel approach in liver cancer therapy. Diss. (2018). Keele University.

[14] Damiri, F., Bachra, Y., Bounacir, C., Laaraibi, A., & Berrada, M. Synthesis and characterization of lyophilized chitosan-based hydrogels cross-linked with benzaldehyde for controlled drug release. Journal of Chemistry, (2020).

[15] Iqbal, D. N., Tariq, M., Khan, S. M., Gull, N., Iqbal, S. S., Aziz, A., ... & Iqbal, M. Synthesis and characterization of chitosan and guar gum based ternary blends with polyvinyl alcohol. International journal of biological macromolecules, (2020).143, 546-554.

[16] Santhosh, A., Theertha, V., Prakash, P., & Chandran, S. S. From waste to a value added product: Green synthesis of silver nanoparticles from onion peels together with its diverse applications. Materials Today: Proceedings.(2020).

[17] El-Borady, O. M., Ayat, M. S., Shabrawy, M. A., & Millet, P. Green synthesis of gold nanoparticles using Parsley leaves extract and their applications as an alternative catalytic, antioxidant, anticancer, and antibacterial agents. Advanced Powder Technology, (2020). 31(10), 4390-4400.

[18] Hassan, O. M., Ibraheem, I. J., Adil, B. H., Obaid, A. S., & Salih, T. A. Synthesis of Silver Nanoparticles by ecofriendly nvironmental method using Piper nigrum, Ziziphus spina-christi, and Eucalyptusglobulus extract. In Journal of Physics: Conference Series (2020). (Vol. 1530, No. 1, p. 012139).

[19] Hezma, A. M., Rajeh, A., & Mannaa, M. A. An insight into the effect of zinc oxide nanoparticles on the structural, thermal, mechanical properties and antimicrobial activity of Cs / PVA composite. Colloids and Surfaces A: Physicochemical and Engineering Aspects, (2019). 581, 123821.

[20] Murali, S., Kumar, S., Koh, J., Seena, S., Singh, P., Ramalho, A., & Sobral, A. J. Bio-based chitosan / gelatin / Ag@ ZnO bio nanocomposites: synthesis and mechanical and antibacterial properties. Cellulose, (2019). 26(9), 5347-5361.

[21] Al-Ziaydi, A. G., Al-Shammari, A. M., Hamzah, M. I, and Jabir, M. S. Hexokinase inhibition using D-Mannoheptulose enhances oncolytic newcastle disease virus-mediated killing of breast cancer cells. Cancer Cell International, (2020). 20(1), 1-10.

[22] Al-Ziaydi, A. G., Hamzah, M. I., Al-Shammari, A. M., Kadhim, H. S., and Jabir, M. S. The anti-proliferative activity of D-mannoheptulose against breast cancer cell line through glycolysis inhibition. In AIP Conference Proceedings (2020). (Vol. 2307, No. 1, p. 020023). AIP Publishing LLC.

[23] Al-Salman, H. N. K., Ali, E. T., Jabir, M., Sulaiman, G. M., and Al-Jadaan, S. A. 2-Benzh-ydrylsulfinyl-N-hydroxya cetamide-Na extracted from fig as a novel cytotoxic and apoptosis inducer in SKOV-3 and AMJ-13 cell lines via P53 and caspase-8 pathway. Eurpean food research and technology. (2020).

[24] Al-Ziaydi, A. G., Al-Shammari, A. M., Hamzah, M. I., Kadhim, H. S., and Jabir, M. S. Newcastle disease virus suppress glycolysis pathway and induce breast cancer cells death. Virus Disease, (2020). 1-8.

[25] Kareem, S. H., Naji, A. M., Taqi, Z. J., and Jabir, M. S. Polyvinylpyrrolidone Loaded-$MnZnFe_2O_4$ Magnetic Nanocomposite Induce Apoptosis in Cancer Cells Through Mitochondrial Damage and p 53 pathway. Journal of Inorganic and Organometallic polymers and materials, (2020). 1-15.

[26] Jabir, M. S., Hussien, A. A., Sulaiman, G. M., Yaseen, N. Y., Dewir, Y. H., Alwahibi, M. S., ... and Rizwana, H. Green synthesis of silver nanoparticles from Eriobotrya japonica extract: a promising approach against cancer cells proliferation, inflammation, allergic disorders and phagocytosis induction. Artificial Cells, Nanomedicine, and Biotechnology, (2021). 49(1), 48-60.

[27] Al-Shammari, A. M., Al-Saadi, H., Al-Shammari, S. M., and Jabir, M. S. Galangin enhances goldnanoparticles as anti-tumor agents against ovarian cancer cells. In AIP Conference Proceedings (2020). (Vol. 2213, No 1, p. 020206). AIP Publishing LLC.

[28] Majid S. Jabir, Yasmin M. Saleh, Ghassan M. Sulaiman, Nahi Y. Yaseen, Usama I. Sahib, Yaser Hassan Dewir , Mona S. Alwahibi and Dina A. Soliman Green Synthesis of Silver Nanoparticles Using Annona muricata Extract as an Inducer of Apoptosis in Cancer Cells and Inhibitor for NLRP3 Inflammasome via Enhanced Autophagy. Nanomaterials. (2021). 11, 384. 1-22.

[29] Khashan, K. S., Abdulameer, F. A., Jabir, M. S., Hadi, A. A., and Sulaiman, G. M. Anticancer activity and toxicity of carbon nanoparticles produced by pulsed laser ablation of graphite in water. Advances in Natural Sciences: Nanoscience and Nanotechnology, (2020). 11(3), 035010.

[30] Jabir, M., Sahib, U. I., Taqi, Z., Taha, A., Sulaiman, G., Albukhaty, S., ... and Rizwana, H. Linalool-Loaded

Glutathione-Modified Gold Nanoparticles Conjugated with CALNN Peptide as Apoptosis Inducer and NF-κB Translocation Inhibitor in SKOV-3 Cell Line. International Journal of Nanomedicine, (2020). 15, 9025.

[31] Sameen, A. M., Jabir, M. S., andAl-Ani, M. Q. Therapeutic combination of gold nanoparticles and LPS as cytotoxic and apoptosis inducer in breast cancer cells. In AIP Conference Proceedings(2020). (Vol. 2213, No. 1, p. 020215). AIP Publishing LLC.

[32] Mathew, B.; Joseph, S.; Koshy, E.P.; Mathew, B. Green synthesis and characterization of gold and silvernanoparticles using Mussaenda glabrata leaf extract and their environmental applications to dye degradation. Environ, Sci. Pollut. Res. (2017). 24, 17347–17357.

[33] Raj, S.; Mali, S.C.; Trivedi, R. Green synthesis and characterization of silver nanoparticles using Enicostemmaaxillare (Lam.) leaf extract. Biochem. Biophys. Res. Commun. (2018). 503, 2814–2819.

[34] Khalil T. Hassan and etc. " Facile green synthesis of Ag/AgCl nanoparticles derived from Chara algae extract and evaluating their antibacterial activity and synergistic effect with antibiotics" Journal of Environmental Chemical Engineering 9 (2021).

[35] Soshnikova, V.; Kim, Y.-J.; Singh, P.; Huo, Y.; Markus, J.; Ahn, S.; Castro-Aceituno, V.; Kang, J.;Chokkalingam, M.; Mathiyalagan, R.; et al. Cardamom fruits as a green resource for facile synthesisof gold and silver nanoparticles and their biological applications. Artif. Cells Nanomed. Biotechnol. (2017). 46,108–117.

[36] Rajeshkumar, S. "Anticancer activity of eco-friendly gold nanoparticles against lung and liver cancer cells". Journal of Genetic Engineering and Biotechnology, (2016). 14(1), 195-202.

[37] Pokrowiecki, R., Wojnarowicz, J., Zareba, T., Koltsov, I., Lojkowski, W., Tyski, S., and Zawadzki, P. "Nanoparticles and human saliva: A step towards drug delivery systems for dental and craniofacial biomaterials". International journal of nanomedicine, (2019). 14, 9235.

[38] El Hamdaoui, L., El Marouani, M., El Bouchti, M., Kifani-Sahban, F., & El Moussaouiti, M. Thermal Stability, Kinetic Degradation and Lifetime Prediction of Chitosan Schiff Bases Derived from Aromatic Aldehydes. *Chemistry Select*, (2021). *6*(3), 306-317.

[39] L.S. Al Banna, N.M. Salem, A.M. Awwad, Green synthesis of sulfur nanoparticles using Rosmarinus officinalis leaves extract and anti-nematicidal activity against Meloidogyne javanica, Chem. Int. (2020). 6, 137-143.

[40] Yildirim, A., & Bulut, Y. Adsorption behaviors of malachite green by using crosslinked chitosan/polyacrylic acid/bentonite composites with different ratios. Environmental Technology & Innovation, (2020). 17, 100560.

[41] Hadidi, M., Pouramin, S., Adinepour, F., Haghani, S., & Jafari, S. M. Chitosan nanoparticles loaded with clove essential oil: characterization, antioxidant and antibacterial activities. Carbohydrate polymers, (2020). 236, 116075. [

42] Shah, A., Ashames, A. A., Buabeid, M. A., & Murtaza, G. Synthesis, in vitro characterization and antibacterial efficacy of moxifloxacin-loaded chitosan-pullulan-silver-nanocomposite films. Journal of Drug Delivery Science and Technology, (2020). 55, 101366.

[43] Furqon, I. A., Hikmawati, D., Abdullah, C., & Azurahanim, C. Antibacterial Properties of Silver Nanoparticle (AgNPs) on Stainless Steel 316L. *Nanomedicine Research Journal*, (2021). *6*(2), 117-127.

[44] Black J G *Microbiology: principles and application* (NewJersey: Prentice-Hall, Inc.) pp. (1996). 80–82.

[45] Saleh TH, Hashim ST, Malik SN, AL-Rubaii BAL. Down-Regulation of full gene expression by Ag nanoparticles andTiO2 nanoparticles in pragmatic clinical isolates of Proteus mirabilis and Proteus vulgaris from urinary tract infection. Nano Biomed Eng.2019; 11(4):321-332.

[46] Ali MAM and Al-Rubaii BAL. Study of the Effects of Audible Sounds and Magnetic Fields on Staphylococcus aureus Methicillin Resistance and mecA Gene Expression. Trop J Nat Prod Res. 2021; 5(5):825-830.

[47] Mohamed, N. Synthesis of Hybrid Chitosan Silver Nanoparticles Loaded with Doxorubicin with Promising Anti-cancer Activity. Bio Nano Science, (2020). 10, 758-765.